Theory of the Magnetic Moment in Iron Pnictides

Jiansheng Wu,[1] Philip Phillips,[1] and A. H. Castro Neto[2]

[1]*Department of Physics, University of Illinois at Urbana-Champaign, 1110 West Green Street, Urbana, Illinois 61801, USA*
[2]*Department of Physics, Boston University, 590 Commonwealth Avenue, Boston, Massachusetts 02215, USA*

(Received 14 May 2008; published 15 September 2008)

We show that the combined effects of spin orbit, monoclinic distortion, and p-d hybridization in tetrahedrally coordinated Fe in LaFeAsO invalidate the naive Hund's rule filling of the Fe d levels. The two highest occupied levels have one electron each, but, as a result of differing p-d hybridizations, the upper level is more itinerant, while electrons in the lower level are more localized. The resulting magnetic moment is highly anisotropic with an in-plane value of $0.25\mu_B$–$0.35\mu_B$ per Fe and a z projection of $0.06\mu_B$, both of which are in agreement with experiment.

DOI: 10.1103/PhysRevLett.101.126401 PACS numbers: 71.10.Hf, 71.27.+a, 71.55.−i, 75.20.Hr

The representative parent material LaFeAsO in the rapidly growing class of iron-based superconductors [1–4] exhibits a structural monoclinic distortion from tetragonal symmetry at 150 K followed by a transition to an antiferromagnet [5–8] at 134 K with a unit cell of $(\sqrt{2} \times \sqrt{2} \times 2)$. The observed magnetic moment per Fe atom has been reported to range from $0.25\mu_B$ [8] to $0.36\mu_B$ [5] and lies in the a-b plane. Such a low value of the magnetic moment is astounding, because any application of Hund's rule to the Fe d states results in a moment of at least $2\mu_B$. We offer here a resolution of the low *in-plane* magnetic moment in LaFeAsO which is rooted in three effects that are well known to be important in FeAs-based materials [9–11], namely, spin orbit, strong hybridization between the Fe d and the As $4p$ orbitals, and the lattice compression along the z axis to the lower monoclinic symmetry. All three conspire to destroy the naive Hund's rule filling of the Fe atomic levels as illustrated in Fig. 1.

That the properties of Fe-based materials are strong functions of the hybridization is not new. Well known is the case of an isolated Fe atom which has a moment of $4\mu_B$, whereas in the metal the moment is roughly halved to $2.2\mu_B$ per Fe as a result [12] of the $4s$ and $3d$ hybridization. Less well known, but more pertinent to LaFeAsO, is the case of the zinc blende complex FeAs which is also an antiferromagnet and has a monoclinic distortion [13]. First-principles calculations on Fe films deposited on GaAs [10] reveal that the value of the magnetic moment per Fe is a strong function of the Fe-As bond distance. The moment vanishes [10] for Fe-As distances less than 2.36 Å. This effect was attributed [10] to the strong hybridization between the Fe $3d$ and the As $4p$ orbitals. In LaFeAsO, the average Fe-As bond distance 2.4 Å is close to the critical value of 2.36 Å found for Fe-As films. As the degree to which Fe and As are noncoplanar in FeAs and LaoFeAs is identical, similar extreme sensitivity of the moment to the p-d hybridization is expected in LaFeAsO.

It is ultimately symmetry that dictates hybridization. In LaFeAsO, each Fe is tetrahedrally coordinated. Full tetrahedral (cubic) symmetry splits the d states into two irreducible representations [9,11]: (i) the threefold degenerate Γ_{15} levels consisting of the d_{xy}, d_{yz}, and d_{xz} and (ii) the doubly degenerate Γ_{12} consisting of $d_{x^2-y^2}$ and d_{z^2}. The Γ_{12} levels lie lower in energy. It is important to note that, in a tetrahedral field, only the Γ_{15} states have the right symmetry to hybridize with the p states of the sp neighboring atom, forming bonding and antibonding hybrid orbitals. The Γ_{12} levels remain nonbonding and hence will be neglected in our hybridization analysis. They will be assumed to constitute a full band (4 electrons). The immediate problem with applying Hund's rule to the Γ_{15} levels is that the effective moment on these levels is at least $2\mu_B$ as found in recent calculations [14]. While inclusion of magnetic frustration [15] might offer some reduction in the moment, it offers no resolution of the problem that the moment lies in the xy plane. The answer lies elsewhere as suggested by recent first-principles calculations [16] and a p-d mixing model [17].

The experimental observation that the Fe moment lies in the plane is highly suggestive of spin-orbit coupling. To this end, our starting point is a general model

$$H = \mathbf{p}^2/(2m) + V_0 + \hbar/(4m^2c^2)(\nabla V_0 \times \mathbf{p}) \cdot \vec{\mathbf{S}} \qquad (1)$$

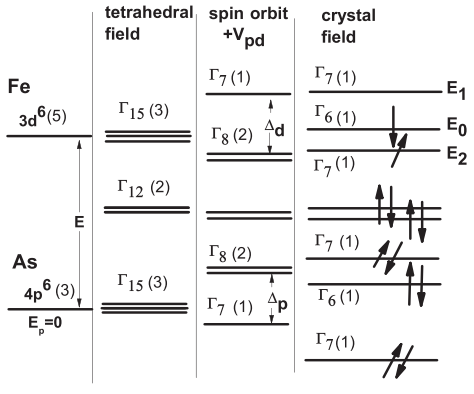

FIG. 1. Evolution of the energy levels of the Fe $3d$ and As $4p$ levels after the inclusion of spin-orbit coupling, p-d hybridization V_{pd}, and the monoclinic crystal field distortion.

for a cubic crystal with spin-orbit interaction, where $\mathbf{p}$ is the momentum operator and $\mathbf{S}$ is the spin operator. This interaction breaks $SU(2)$ symmetry. The rough idea is to include the effects of p-d hybridization and the z axis distortion through a series of successive diagonalizations to obtain the eigenstates in the final basis. We include only the outline of this calculation since an analogous analysis has been done for chalcopyrite semiconductors [9]. In obtaining the basis that diagonalizes the spin-orbit interaction, we define $|\pm\rangle = |(X \pm iY)/\sqrt{2}\rangle$, $|0\rangle = |Z\rangle$, which are eigenstates of angular momentum (L, L_z) with eigenvalues $(1, \pm 1)$ and $(1, 0)$, respectively. The Hamiltonian for the p levels is diagonalized through

$$\begin{aligned}
\phi^{\alpha}_{p1}(\Gamma_8) &= 1/\sqrt{3}|-\uparrow\rangle + \sqrt{2/3}|0\downarrow\rangle (J_z = -1/2),\\
\phi^{\alpha}_{p0}(\Gamma_8) &= |+\uparrow\rangle (J_z = +3/2),\\
\phi^{\alpha}_{p2}(\Gamma_7) &= \sqrt{2/3}|-\uparrow\rangle - 1/\sqrt{3}|0\downarrow\rangle (J_z = -1/2),\\
\phi^{\beta}_{p1}(\Gamma_8) &= -1/\sqrt{3}|+\downarrow\rangle + \sqrt{2/3}|0\uparrow\rangle (J_z = +1/2),\\
\phi^{\beta}_{p0}(\Gamma_8) &= |-\downarrow\rangle (J_z = -3/2),\\
\phi^{\beta}_{p2}(\Gamma_7) &= -\sqrt{2/3}|+\downarrow\rangle - 1/\sqrt{3}|0\uparrow\rangle (J_z = +1/2).
\end{aligned} \tag{2}$$

States with the same indices are degenerate, and Γ_n denotes the symmetry of a state. Likewise, the basis for the d levels which initially have Γ_{15} symmetry

$$\begin{aligned}
\phi^{\alpha}_{d1}(\Gamma_8) &= 1/\sqrt{3}|\ominus\uparrow\rangle + \sqrt{2/3}|\odot\downarrow\rangle (J_z = -1/2),\\
\phi^{\alpha}_{d0}(\Gamma_8) &= |\oplus\uparrow\rangle (J_z = +3/2),\\
\phi^{\alpha}_{d2}(\Gamma_7) &= \sqrt{2/3}|\ominus\uparrow\rangle - 1/\sqrt{3}|\odot\downarrow\rangle (J_z = -1/2),\\
\phi^{\beta}_{d1}(\Gamma_8) &= -1/\sqrt{3}|\oplus\downarrow\rangle + \sqrt{2/3}|\odot\uparrow\rangle (J_z = +1/2),\\
\phi^{\beta}_{d0}(\Gamma_8) &= |\ominus\downarrow\rangle (J_z = -3/2),\\
\phi^{\beta}_{d2}(\Gamma_7) &= -\sqrt{2/3}|\oplus\downarrow\rangle - 1/\sqrt{3}|\odot\uparrow\rangle (J_z = +1/2)
\end{aligned} \tag{3}$$

is formed from the states; $|\oplus\rangle = |(YZ + iZX)/\sqrt{2}\rangle$, $|\ominus\rangle = |(YZ - iZX)/\sqrt{2}\rangle$, and $|\odot\rangle = |XY\rangle$ are the eigenstates of (L, L_z) with eigenvalues of $(2, +1)$, $(2, -1)$, and $(2, 0)$, respectively. As is clear, none of these states is an eigenstate of S_z as is expected once the $SU(2)$ spin symmetry is broken by the spin-orbit interaction.

To consider the hybridization, we collate the states into two groups, segregating them according to their superscript α or β. Within each group they are ordered as follows: $\phi^{\alpha}_{p1}(\Gamma_8)$, $\phi^{\alpha}_{d1}(\Gamma_8)$, $\phi^{\alpha}_{p0}(\Gamma_8)$, $\phi^{\alpha}_{d0}(\Gamma_8)$, $\phi^{\alpha}_{p2}(\Gamma_7)$, and $\phi^{\alpha}_{d2}(\Gamma_7)$. Taking into consideration that only states of the same symmetry mix,

$$\langle \phi^{\alpha}_{\mathrm{pi}}(\Gamma_m)|V_{\mathrm{pd}}|\phi^{\alpha}_{dj}(\Gamma_n)\rangle = M\delta_{ij}\delta_{\alpha\beta}\delta_{mn}, \tag{4}$$

we find that the hybridization matrix can be written as

$$V_{\mathrm{pd}} = \begin{bmatrix}
\frac{\Delta_p}{3} & M & 0 & 0 & 0 & 0\\
M & E - \frac{\Delta_q}{3} & 0 & 0 & 0 & 0\\
0 & 0 & \frac{\Delta_p}{3} & M & 0 & 0\\
0 & 0 & M & E - \frac{\Delta_d}{3} & 0 & 0\\
0 & 0 & 0 & 0 & -2\frac{\Delta_p}{3} & M\\
0 & 0 & 0 & 0 & M & E + 2\frac{\Delta_d}{3}
\end{bmatrix}, \tag{5}$$

where Δ_p and Δ_q are the spin-orbit splitting of the p and d band, respectively. The highest three eigenenergies are

$$\lambda_0 = \lambda_1 = [\Delta_p/3 + E - \Delta_d/3]/2 + \sqrt{\alpha_1}/2, \tag{6}$$

$$\lambda_2 = [-2\Delta_p/3 + E + 2\Delta_d/3]/2 + \sqrt{\alpha_2}/2, \tag{7}$$

where $\alpha_1 = (\Delta/3 - E + \Delta_d/3)^2 + 4M^2$ and $\alpha_2 = (2\Delta/3 + E + 2\Delta_d/3)^2 + 4M^2$. According to the symmetries Γ_n, $n = 7$ or $n = 8$, the corresponding eigenstates are $\Phi^{\alpha}_i(\Gamma_n) = a_i\phi^{\alpha}_{pi}(\Gamma_n) + b_i\phi^{\alpha}_{di}(\Gamma_n)$, with the coefficients a_i $(i = 0, 1, 2)$ and b_i defined as

$$\gamma_0 = \gamma_1 = a_1^2 = 1 - b_1^2 = [1 + M^2/(\lambda_1 - E + \Delta_d/3)^2]^{-1},$$
$$\gamma_2 = a_2^2 = 1 - b_2^2 = [1 + M^2/(\lambda_2 - E - 2\Delta_d/3)^2]^{-1}.$$

To gain information about the spins, we transform the operator for the z projection of the spin

$$\sigma_z^{I_\alpha} = \frac{1}{3}\begin{bmatrix}
-1 & 0 & 0 & 0 & 2\sqrt{2} & 0\\
0 & -1 & 0 & 0 & 0 & 2\sqrt{2}\\
0 & 0 & 3 & 0 & 0 & 0\\
0 & 0 & 0 & 3 & 0 & 0\\
2\sqrt{2} & 0 & 0 & 0 & 1 & 0\\
0 & 2\sqrt{2} & 0 & 0 & 0 & 1
\end{bmatrix} \tag{8}$$

and $\sigma_z^{I_\beta} = -\sigma_z^{I_\alpha}$ into the I_α or I_β basis.

Ultimately, we will focus only on the three highest eigenstates. We refer to this reduced basis as $II^{\alpha,\beta}$. The final ingredient is the z axis distortion from perfect cubic symmetry. We consider a crystal field interaction of the form

$$\begin{aligned}
\langle X|V_{\mathrm{cf}}|X\rangle &= \zeta\langle Y|V_{\mathrm{cf}}|Y\rangle = \delta_p/3,\\
\langle Z|V_{\mathrm{cf}}|Z\rangle &= -2\delta_p/3,\\
\langle ZX|V_{\mathrm{cf}}|ZX\rangle &= \zeta\langle YZ|V_{\mathrm{cf}}|YZ\rangle = \delta_d/3,\\
\langle XY|V_{\mathrm{cf}}|XY\rangle &= -2\delta_p/3.
\end{aligned}$$

The parameter ζ accounts for the distortion in the a-b plane. Experimentally, the lattice constants along a and b differ by 0.3%. While any distortion is sufficient to lower the $U(1)$ rotational symmetry in the plane to simply Z_2 (Ising), this effect is small relative to the overall z axis tilt. As the parameter δ_p is certainly not known within 0.3%, we consider only the case of $\zeta = 1$. The crystal field Hamiltonian in the $II^{\alpha,\beta}_R$ is

$$V_{\rm cf} = \begin{bmatrix} \lambda_1 - \Gamma_1 & 0 & \Gamma_2 \\ 0 & \lambda_0 + \Gamma_1 & 0 \\ \Gamma_2 & 0 & \lambda_2 \end{bmatrix}, \quad (9)$$

where $\Gamma_1 = \frac{1}{3}[\delta_p\gamma_1 + \delta_d(1-\gamma_1)]$ and $\Gamma_2 = \frac{\sqrt{2}}{3} \times [\delta_p\sqrt{\gamma_1\gamma_2} + \delta_d\sqrt{(1-\gamma_1)(1-\gamma_2)}]$. Diagonalizing this Hamiltonian gives rise to the following three energy levels: $E_0(\Gamma_6) = \lambda_0 + \Gamma_1$ and

$$2E_{1,2}(\Gamma_7) = \lambda_1 + \lambda_2 - \Gamma_1 \pm \sqrt{(\lambda_1 - \lambda_2 - \Gamma_1)^2 + 4\Gamma_2^2}$$

and their corresponding eigenstates

$$\Psi_0^{\alpha,\beta}(\Gamma_6) = \Phi_0^{\alpha,\beta}(\Gamma_7), \quad (10)$$

$$\Psi_i^{\alpha,\beta}(\Gamma_7) = c_1\Phi_i^{\alpha,\beta}(\Gamma_8) + d_1\Phi_i^{\alpha,\beta}(\Gamma_7), \quad (11)$$

which we refer to as the $III^{\alpha(\beta)}$ basis, where $i = 1, 2$ and c_i and d_i are defined as $c_1^2 = 1 - d_1^2 = 1/[1 + \Gamma_2^2/(E_1 - \lambda_2)]$, with $d_2 = -c_1$, and $c_2 = d_1$. In the final basis $III^{\alpha(\beta)}$, the σ_z spin matrix becomes

$$\sigma_z^{III_R^\alpha} = -\sigma_z^{III_R^\beta} = \begin{bmatrix} e & 0 & f \\ 0 & 1 & 0 \\ f & 0 & -e \end{bmatrix}, \quad (12)$$

where $e = 2c_1d_1\Gamma + (d_1^2 - c_1^2)/3$, $f = (d_1^2 - c_1^2)\Gamma - 2c_1d_1/3$, and $\Gamma = 2\sqrt{2}(a_1a_2 + b_1b_2)/3$. So we can see clearly that the final basis does not diagonalize the spin matrix. Consequently, the states $III^{\alpha(\beta)}$ represent some linear combination of spin up and spin down. A crucial point about this spin matrix: The α and β states have opposite projections of spin in the states with energies E_1 and E_2.

In the transformed basis, the resultant Hamiltonian reads

$$H = \sum_{a,\mu,i} E_a c^\dagger_{a,\mu,i} c_{a,\mu,i} - \sum_{a,b,\mu,\nu,\langle i,j\rangle} t^{\mu,\nu}_{a,b} c^\dagger_{a,\mu,i} c_{b,\nu,j} + \text{H.c.} + \sum_{a,b\mu,\nu,i} U^{\mu\nu}_{ab} n_{ia\mu} n_{ib\nu}, \quad (13)$$

where $a, b = 0, 1, 2$ and $\mu, \nu = \alpha, \beta$, and

$$\begin{aligned}
t_0 &= t_{00}^{\alpha\alpha} = t_{00}^{\beta\beta} = a_1^4 t_p + b_1^4 t_d, \\
t_1 &= t_{11}^{\alpha\alpha} = t_{11}^{\beta\beta} = (c_1^2a_1^2 + d_1^2a_2^2)t_p + (c_1^2b_1^2 + d_1^2b_2^2)t_d, \\
t_2 &= t_{22}^{\alpha\alpha} = t_{22}^{\beta\beta} = (d_1^2a_1^2 + c_1^2a_2^2)t_p + (d_1^2b_1^2 + c_1^2b_2^2)t_d, \\
t_{12} &= t_{12}^{\alpha\beta} = c_1d_1(a_1^2 - a_2^2)t_p + c_1d_1(b_1^2 - b_2^2)t_d, \\
U_0^{\alpha\beta} &\equiv U_{00}^{\alpha\beta} = a_1^4U_p/2 + b_1^4U_d/2, \\
U_i^{\alpha\beta} &= (C_i^4 + A_i^4/2)U_p + (D_i^4 + B_i^4/2)U_d, \qquad (i = 1, 2) \\
U_{12}^{\alpha\beta} &= [(C_1C_2)^2 + A_1A_2)^2/2]U_p \\
&\quad + [(D_1D_2)^2 + (B_1B_2)^2/2]U_d, \\
U_{0i}^{\alpha\beta} &= (a_1A_i)^2U_p/2 + (b_1B_i)^2U_d/2 (i = 1, 2). \quad (14)
\end{aligned}$$

All other couplings, for example, t_{01} and t_{02}, vanish by symmetry. The coefficients A_i, B_i, C_i, and D_i are defined as

$$\begin{aligned}
A_i &= 1/\sqrt{3}c_ia_1 + \sqrt{2/3}d_ia_1, \\
B_i &= 1/\sqrt{3}c_ib_1 + \sqrt{2/3}d_ib_1, \\
C_i &= \sqrt{2/3}c_ia_1 - 1/\sqrt{3}d_ia_1, \\
D_i &= \sqrt{2/3}c_ib_1 - 1/\sqrt{3}d_ib_1,
\end{aligned}$$

where c_1, d_1, a_i, and b_i are defined as before.

We analyzed the energy levels, interaction strengths, and spin projections based on representative values for iron-based systems. For instance, if we set $U_p = U_d = 4$ eV [18], $t_p = t_d = 0.7$ eV [14,18], $M = 0.8$ eV [14,15], $\Delta_p = 0.426$ eV [19], $\Delta_d = 0.08$ eV [12], $E = 1.9$ eV [14], and $\delta_p = \delta_d = 0.06$ eV [20], we arrive at the parameters of Table I for Hamiltonian (13). Notice, however, that there is an uncertainty in the value of these parameters, especially the hybridization energy M and the monoclinic distortion. Hence, we explore the dependence of the Hamiltonian parameters on both. As shown in the first panel of Fig. 2(a), the E_2 level is the lowest followed by E_0 and then E_1 for sufficiently large values of M. As can be seen from Fig. 2(b), $U_2 > E_0 - E_2$ and $E_1 - E_2$. Consequently, E_2 and one of E_0 or E_1 will be singly occupied. To determine the ground state spin configuration, we note that both the interactions $U_{12}^{\alpha\beta} \neq 0$ and $U_{02}^{\alpha\beta} \neq 0$ [see Fig. 2(c)] with $\alpha \neq \beta$ for the highest two occupied levels. Recall that the z projection of the spins in α and β is reversed in levels E_0 (or E_1) relative to E_2. Level E_0 is an eigenstate of S_z, while E_1 is not. Consequently, the lowest-energy configuration for single occupancy of the levels E_0 and E_2 is an antiparallel alignment of the spins. That is, both electrons are in the α or in the β state in both levels. This configuration does not cost the repulsion term $U_{02}^{\alpha\beta}$ or $U_{12}^{\alpha\beta}$. Since there are 12 electrons to fill these levels, we arrive at the filling structure shown in Fig. 1. Consequently, the three effects considered preclude a naive assignment of the spins according to Hund's rule [17]. This conclusion is a general result of this analysis, not an artifact of fine-tuning the bare parameters.

The problem has now been reduced to the physics of two low-lying energy levels E_1 and E_2. That a two-band reduction reproduces [21] the Fermi surface seen in the local density approximation [22] and experiments [23] corroborates our approach. If we neglect the interactions in (13), the problem can be easily diagonalized, and one finds two, doubly degenerate, energy-shifted bands. The splitting between the bands is due to the crystal field that shifts

TABLE I. Energy levels, hopping matrix elements, and interactions in the three highest levels in transformed basis $III^{\alpha(\beta)}$.

$\delta_{p(d)}$	E_0	E_1	E_2	$t_{0(1,2)}$	$t_{12}^{\alpha\beta}$	U_0	U_1	U_2	U_{12}	U_{01}	U_{02}
0.06	2.21	2.22	2.15	0.7	0	1.54	1.55	2.98	0.12	1.54	0.035
0	2.22	2.21	2.19	0.7	0	1.54	1.11	1.54	1.07	1.07	0.51

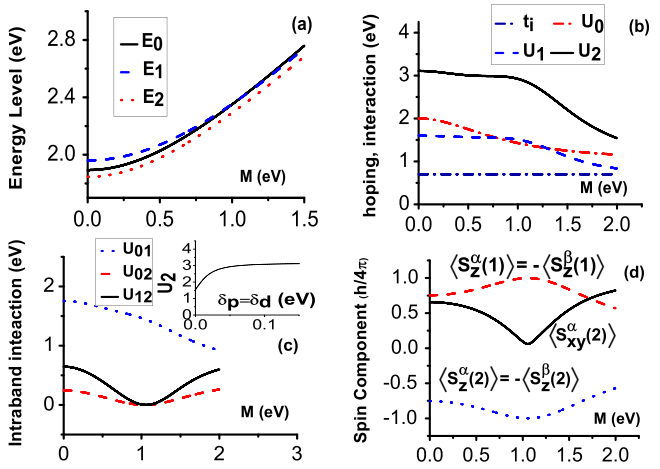

FIG. 2 (color online). Energy levels, hoping matrix elements, on-site interactions, intraband interaction, and spin components as a function of hybridization M. Shown in the inset of (c) is the on-site interaction U_2 as a function of the monoclinic distortion.

each half-filled band away from the perfect nesting condition. As a result, it is difficult to reconcile the experimental observation of a spin-density wave with a simple Fermi surface instability due to nesting. The resolution may lie in the interactions. As Fig. 2(b) indicates, for all values of the hybridization, levels 1 and 2 have differing p and d character. In E_2 the on-site interaction, U_2 exceeds U_0 (or U_1) by more than a factor of 2 at $M = 0.8$ eV. Consequently, single occupancy in the E_0 (or the E_1) level results in itineracy, whereas in the E_2 level Mott physics can be relevant since $U_2 \approx 4t_2$. This difference is due entirely to the different p-d character between the E_0 (or E_1) and E_2 levels which is expected as they are orthogonal. Finally, we show in the last panel in Fig. 2(d) the value of S_z in levels E_1 and E_2. Recall that level E_0 is an eigenstate of S_z with the z projection opposite to that in E_2. As shown in the last panel in Fig. 2, the value of S_z in E_2 is $0.95\mu_B$. If E_0 is the next lowest level, a net moment in the z direction of $0.06\mu_B$ remains as has been recently observed [7]. If E_1 is relevant (as would be the case for $M > 0.83$ eV), the z moment vanishes as shown in Fig. 2(d). The itineracy of the electrons in the E_0 level does not affect this cancellation as it is the average not the local spin configuration that is relevant in a magnetization measurement. Hence, for experimentally relevant values of M (0.5 eV $< M <$ 1.0 eV), the residual z component of the moment is strongly diminished. The remaining x-y component on E_2 is $S_{xy} = \sqrt{1 - \langle S_z \rangle^2} = 0.317\mu_B$. Such a moment can order via the superexchange mechanism on E_2 as $U_2 \gg t_2$. The evolution of S_{xy} as a function of M in Fig. 2(d) shows that the analysis here is consistent with the range of the magnetic moment seen experimentally [5,8].

Our analysis also explains why the structural transition [5] at 150 K must precede the onset of antiferromagnetism. As the inset in Fig. 2(c) indicates, the on-site energy U_2 diminishes as the crystal field associated with the monoclinic distortion vanishes. Once $U_2 < t_2$, a transition to an antiferromagnet via the superexchange interaction is untenable. The structural transition breaks rotational symmetry in the plane not $SU(2)$ which is already broken at the outset by spin-orbit interaction. The success of the analysis presented here in describing the antiferromagnet in the parent material LaFeAsO implies that Eq. (13) should be used in any subsequent analysis of superconductivity. The presence of an itinerant band coupled to one with moderate Mott physics makes the problem of the iron pnictides more akin [24] to that of the Kondo lattice in heavy fermions than the cuprates.

This work was supported by the NSF, Grant No. DMR-0605769.

Note added.—While this work was under review, McGuire *et al.* [7] reported a residual magnetic moment along the c axis equal to $0.06\mu_B$ as predicted here.

[1] Y. Kamihara *et al.*, J. Am. Chem. Soc. **130**, 3296 (2008).
[2] J. Yang *et al.*, Supercond. Sci. Technol. **21**, 082001 (2008).
[3] P. C. Cheng *et al.*, arXiv:0804.08352.
[4] Z.-A. Ren *et al.*, Mater. Res. Innovations **12**, 1 (2008).
[5] C. de la Cruz *et al.*, Nature (London) **453**, 899 (2008).
[6] J. Dong *et al.*, arXiv:0803.3426.
[7] M. A. McGuire *et al.*, arXiv:0806.3878.
[8] H.-H. Klauss *et al.*, Phys. Rev. Lett. **101**, 077005 (2008).
[9] K. Yoodee, J. C. Woolley, and V. Sa-yakanit, Phys. Rev. B **30**, 5904 (1984).
[10] S. Mirbt *et al.*, Phys. Rev. B **67**, 155421 (2003).
[11] I. Galanakis and P. Mavropoulos, Phys. Rev. B **67**, 104417 (2003).
[12] M. L. Tiago *et al.*, Phys. Rev. Lett. **97**, 147201 (2006).
[13] H. Katsuraki and N. Achiwa, J. Phys. Soc. Jpn. **21**, 2238 (1952); N. Achiwa *et al.*, J. Phys. Soc. Jpn. **22**, 156 (1953).
[14] C. Cao, P. J. Hirschfeld, and H.-P. Cheng, Phys. Rev. B **77**, 220506(R) (2008).
[15] Q. Si and E. Abrahams, Phys. Rev. Lett. **101**, 076401 (2008).
[16] Y. Yildirim, Phys. Rev. Lett. **101**, 057010 (2008).
[17] V. Cvetkovic and Z. Tesanovic, arXiv:0804.4678.
[18] K. Haule, J. H. Shim, and G. Kotliar, Phys. Rev. Lett. **100**, 226402 (2008).
[19] F. Herman *et al.*, Phys. Rev. Lett. **11**, 541 (1963).
[20] A. O. Shorikov *et al.*, arXiv:0804.3283v1.
[21] S. Raghu *et al.*, Phys. Rev. B **77**, 220503(R) (2008).
[22] D. J. Singh and M. H. Du, Phys. Rev. Lett. **100**, 237003 (2008).
[23] A. I. Coldea *et al.*, arXiv:0807.4890.
[24] G. Giovannetti, S. Kumar, and J. van den Brink, arXiv:0804.0866.